International Journal of Thermophysics, Vol. 24, No. 3, May 2003 (© 2003)

Development of Spectral Selective Multilayer Film for a Variable Emittance Device and Its Radiation Properties Measurements[1]

K. Shimazaki,[2,3] A. Ohnishi,[4] and Y. Nagasaka[5]

A smart radiation device (SRD) that is a variable emittance radiator has been developed as a thermal control material for spacecraft. The SRD has the unique feature of large variation of the total hemispherical emittance ε_H near room temperature. The ε_H of the SRD changes depending on its temperature. However, there is a drawback of a large solar absorptance α_S. It is too large to use as a thermal control material for spacecraft. In order to reduce the large α_S, spectral selective multilayer film was developed. This multilayer film reflects solar radiation and transmits far-infrared radiation to maintain the variation in the ε_H of the SRD. This paper presents thermal radiative properties of the SRD with spectral selective multilayer film. The multilayer film was designed by using a genetic algorithm (GA). The designed multilayer film was evaporated on the surface of the SRD by the electron beam evaporation method. The experimental results of α_S and ε_H of the SRD with the multilayer film agreed well with calculated results.

KEY WORDS: genetic algorithm; $La_{1-x}Sr_xMnO_3$; manganese oxide; multilayer films; optical constants; solar absorptance; spectral reflectance; total hemispherical emittance.

[1] Paper presented at the Sixteenth European Conference on Thermophysical Properties, September 1–4, 2002, London, United Kingdom.

[2] Graduate School of Science and Technology, Keio University, 3-14-1 Hiyoshi, Yokohama 223-8522, Japan.

[3] To whom correspondence should be addressed. E-mail: kazunori@pub.isas.ac.jp

[4] The Institute of Space and Astronautical Science, 3-1-1 Yoshinodai, Sagamihara 229-8510, Japan.

[5] Department of System Design Engineering, Keio University, 3-14-1 Hiyoshi, Yokohama 223-8522, Japan. E-mail: nagasaka@sd.keio.ac.jp

0195-928X/03/0500-0757/0 © 2003 Plenum Publishing Corporation

1. INTRODUCTION

A wide variety of thermal control materials or devices have been used to achieve the appropriate temperature of spacecraft for all mission phases. However, to solve the problem of complex and variegated thermal designs of the spacecraft, it is desired to develop new functional thermal control materials.

A smart radiation device (SRD) has been developed in recent years [1]. The total hemispherical emittance ε_H of the SRD changes depending on its temperature, with abrupt changes in the vicinity of the metal-insulator transition [2]. The range of the variation in ε_H is more than 0.40. The SRD, however, has a serious problem of a very large solar absorptance, i.e., $\alpha_S > 0.80$. When the SRD is exposed to solar radiation, the temperature of the SRD increases rapidly. Such an abrupt increase of the temperature can cause problems on the spacecraft. To yield a small α_S for the SRD, we designed and applied multilayer films to coat the SRD. The main feature of the multilayer film design is the spectral selectivity of reflecting solar radiation and transmitting far-infrared radiation in order to maintain the variation in the ε_H of the SRD.

In this work, the design of multilayer films for the SRD utilizes optical properties from the ultraviolet to the far-infrared regions because the optical properties of the materials are very different for this wide spectral region, and we must simultaneously determine the solar absorptance and infrared emittance. The present design, furthermore, has to optimize the construction parameters including the thickness and sequence of the materials of the multilayer systems. An important aspect of modern multilayer films design is the use of computers to match the multilayer parameters to a set of optical specifications such as a desired reflectance curve [3, 4]. Therefore, a genetic algorithm (GA) [5] was employed to search for the optimum sequence of the materials along with the thickness of the multilayer films for the SRD. In accordance with the result of the design based on the GA, we evaporated the designed multilayer film on the SRD by the electron beam evaporation method.

In this paper, we briefly introduce the calculation method for thermal radiative properties and the use of the GA for designing multilayer films with the desired thermal radiative properties. In addition, results of the calculated and measured thermal radiative properties of the SRD with the designed multilayer film are presented.

2. CHARACTERISTICS OF SMART RADIATION DEVICE

The smart radiation device (SRD) is made of manganese oxide, polycrystalline $La_{0.825}Sr_{0.175}MnO_3$, with perovskite-type structure. These perovskite-type manganites have recently attracted much attention because

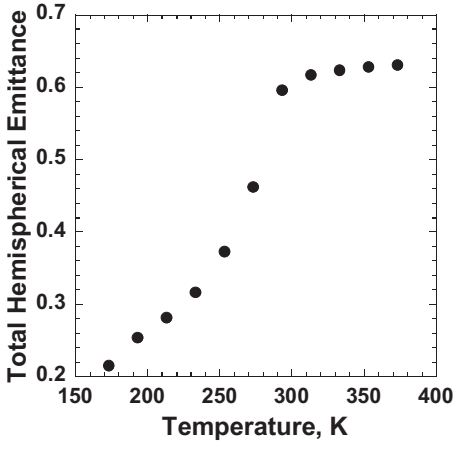

Fig. 1. Temperature dependence of ε_H of SRD.

of giant magnetoresistance phenomena, ferromagnetic transitions, metal-insulator transitions, etc. [6–8]. The performance of the SRD is based on the metal-insulator transition that occurs near room temperature.

The SRD was prepared using the standard ceramic production process [9]. The fundamental dimensions of the SRD are approximately 30 mm × 30 mm × 0.2 mm. The surfaces of every sample were polished with diamond slurry. The surface roughness of the sample was measured with a surface roughness measuring instrument (Tokyo Seimitsu CO., LTD.: SURFCOM 130A). The root-mean-square roughness of the sample is less than 30 nm.

Figure 1 shows ε_H of the SRD in the temperature range from 173 to 373 K. The ε_H of the SRD changes at about 280 K and it decreases at temperatures less than room temperature. Namely, on the one hand, ε_H maintains its high value above 280 K due to insulator-like behavior; on the other hand, it sharply decreases below 280 K because of metallic behavior. The range of the variation in ε_H is more than 0.40.

The solar absorptance α_S of the SRD is 0.81 because of the small spectral reflectance in the spectral region 0.25 to 2.5 μm. This value is too large to use the SRD on the panel that is exposed to solar radiation.

3. MULTILAYER FILM DESIGN

3.1. Application of a Genetic Algorithm to Multilayer Film Design

In the design process of the multilayer films, designers have to determine the appropriate thickness of each layer and the sequence of the

materials in accordance with the design specifications for the optical properties. A genetic algorithm (GA) is of special interest in the field of multilayer film design because such an algorithm can easily incorporate both continuous optimization variables, such as the thickness of the layers, and discrete variables, such as the sequence of the materials used for the different layers [10]. A GA does not require a good starting design to ensure convergence, since it is not easily trapped in a local optimum, which sets it apart from classical iterative techniques [3, 4]. With a GA, there are no assumptions with regard to a necessary sequence of materials. In the present study, a GA was employed for multilayer film design in order to determine the optimal sequence of materials of a particular thickness. A detailed explanation for a GA is given, for example, in Ref. 5.

The GA imitates some of nature's evolutionary principles. A population of coded strings, so-called individuals, develops over time. An individual has $2m$ parameters, i.e., a range of the thickness and a selection of the materials are specified for each of the m layers of a stack. The $2m$-dimensional parameter of the individual is expressed as follows:

$$P = P(d_1, M_1;\ldots; d_m, M_m) \tag{1}$$

where d_m denotes the geometric thickness and M_m denotes the material of the mth layer as shown in Fig. 2. These coded strings determine the structures of the multilayer films of each individual. Every individual is assigned a fitness value that is the linearly scaled merit function value. A new generation of the population is a construct from the old generation by genetic operations. By the crossover operation in the optimization process, the coded strings of an individual are mixed with the coded strings of another individual. Some strings in new individuals are changed at random by the operation of the mutation. If the mth material is changed, the mth thickness is simultaneously changed to avoid production of a stack of poor quality. The main characteristic of the GA is that individuals with a relatively better performance, i.e., with a higher fitness value, have greater probability to survive. Other individuals tend to disappear slowly. The operation of the mutation prevents the algorithm from converging too quickly to a local optimum.

The geometric thickness of the layers was allowed to vary in 10 nm steps in the range of 0 to 300 nm. The maximum number of the layers was set to be 10. If the maximum number of the layers was small, the α_S did not reduce to an acceptable level. If the maximum number of the layers was too large, the variation in ε_H of the SRD became small and it was difficult to find the optimum solution. We employed real codes, and the materials were mapped to integer numbers. In the calculations, a population of 20

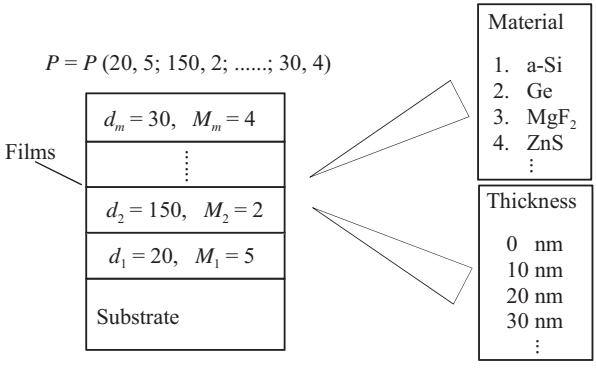

Fig. 2. Schematic drawing of coding.

individuals was processed over 5,000 generations, which means a total of 100,000 function evaluations. Furthermore, we utilized tournament selection, for which the tournament size was 4 with a one-point crossover. The probability of crossover was 0.8. The probability of mutation was 0.1. These parameters of the genetic operations were determined by trials of the optimization for simple multilayer models. In addition, an elite preserving selection (i.e., that the best individual of the old generation replaces an individual of the new generation) was used. All new individuals, except for the elite individual, were completely selected from among the old individuals after the genetic operations were carried out.

3.2. Calculation Method for Thermal Radiative Properties

In the following, we give a short description of the calculation method for thermal radiative properties by use of the optical constants, refractive index n, and extinction coefficient k, of the materials [11]. As thin films are considered in this calculation, assumptions are smooth surfaces and homogeneous, nonscattering materials.

The total hemispherical emittance ε_{H} and solar absorptance α_{S} are calculated from the spectral reflectance. When an interference phenomenon is considered (Fig. 3), the amplitude reflectances which take account of multiple reflection at the boundary surface between the mth and $(m+1)$th layers counted from the bottom of the stack are expressed by a recursion equation as follows [12]:

$$R'_m(\lambda, \theta) = \frac{r_m + R'_{m-1}(\lambda, \theta) \exp(-i\eta_m)}{1 + r_m R'_{m-1}(\lambda, \theta) \exp(-i\eta_m)} \tag{2}$$

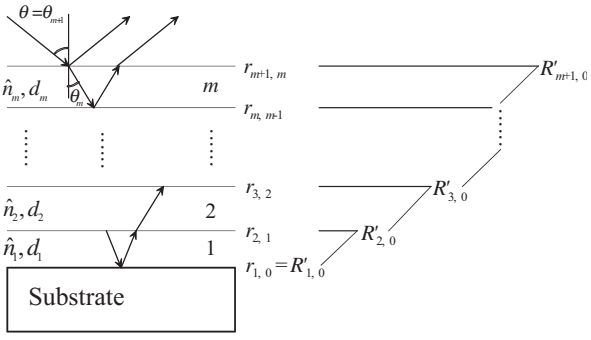

Fig. 3. Schematic drawing of the multiple reflections in the multilayer film.

where $\eta_m = 4\pi\hat{n}_m d_m \cos\theta_m/\lambda$, $\cos\theta_m$ is expressed by the incident angle $\theta = \theta_{m+1}$ of the top layer and the Snell's law. θ_m is a complex number and therefore does not represent the angle of refraction, except for the special case $\theta = 0$. d_m is the geometric thickness, and $\hat{n}_m$ is the complex refractive index of the mth layer. The real part and imaginary part of the complex refractive index are refractive index n and extinction coefficient k, respectively. r_m represents the Fresnel coefficients. Thus, the spectral reflectance of the multilayer films as a function of the incident angle θ and the wavelength λ is expressed by

$$R(\lambda, \theta) = \frac{|R'_{S(m+1)}|^2 + |R'_{P(m+1)}|^2}{2} \tag{3}$$

where $R'_{S(m+1)}$ and $R'_{\rho(m+1)}$ are the amplitude reflectance of S-polarization and P-polarization, respectively, of the surface of the multilayer films. In the present study, the spectral transmittance of the SRD is not considered because the SRD is opaque in the spectral region of 0.25 to 100 μm. By use of a spectroscope, it was confirmed that the SRD is opaque from 0.25 to 100 μm although the thickness of the SRD is only 0.2 mm.

The temperature dependence of ε_H is calculated by integration of the spectral reflectance in the spectral region of 0.25 to 100 μm, expressed by

$$\varepsilon_H(T) = \frac{\int_0^{\pi/2}\int_{0.25}^{100}\{1-R(\lambda,\theta)\}\, i_b(\lambda, T)\cos\theta\sin\theta\, d\lambda\, d\theta}{\int_0^{\pi/2}\int_{0.25}^{100} i_b(\lambda, T)\cos\theta\sin\theta\, d\lambda\, d\theta} \tag{4}$$

where T is the sample temperature and $i_b(\lambda, T)$ is the spectral intensity of a blackbody at temperature T. This spectral region 0.25 to 100.0 μm contains

about 98.0% of the emissive power of the blackbody at 173.15 K, and over 99.0% at 373.15 K.

The α_S is obtained by Eq. (5) using the reflectance data in the spectral region of 0.25 to 2.5 μm as follows:

$$\alpha_S = \frac{\int_{0.25}^{2.5} \{1 - R(\lambda, \theta)\} I_S(\lambda)\, d\lambda}{\int_{0.25}^{2.5} I_S(\lambda)\, d\lambda} \tag{5}$$

where I_S is the intensity of solar radiation [13]. This spectral region 0.25 to 2.5 μm contains approximately 96% of the intensity of solar radiation.

3.3. Optical Constants

In order to design the multilayer films with desired thermal radiative properties, dispersiveness and absorption of the materials from the ultraviolet to the far-infrared regions must be considered. For calculation of ε_H, optical constants of the SRD, n and k, were calculated from Kramers–Kronig (K–K) analysis [14, 15] of the spectral reflectance data from 1.0 to 100 μm including the temperature dependence. The reason for using the temperature dependence of the optical constants of the SRD is that the optical properties of the SRD vary widely, depending on its temperature as shown in Fig. 4 [16]. To calculate the α_S, we used the optical constants of the SRD from 0.25 to 2.5 μm. The optical constants from 0.25 to 1.0 μm were measured by spectral ellipsometry at room temperature, and the optical constants from 1.0 to 2.5 μm were calculated by K–K analysis. Calculation of the α_S was carried out by use of only the data obtained at room temperature because the variation in spectral reflectance of the SRD in the visible region was much smaller than that in the far-infrared region.

As candidate materials for the multilayer films, a-Si, Ge, LiF, MgF_2, ZnS, and ZnSe were selected for the optimization. Their optical constants were basically referenced to the data in the literature [17]. The optical constants of thin films of a-Si and Ge were measured by spectral ellipsometry from 0.25 to 1.70 μm because their optical constants are easily affected by the evaporation condition and are different from the data of the literature. From 1.70 to 100 μm, we assumed that their refractive indices were constant values and their extinction coefficients were 0 because they were transparent in this spectral region. The refractive indices of a-Si and Ge hardly depend on wavelength in the infrared region [17]. The extinction coefficients in the infrared region of a-Si and Ge are negligible in the present calculation because their values are sufficiently small [17]. The optical constants of all candidate materials were considered to be independent of temperature but dispersive and absorptive. This assumption is valid

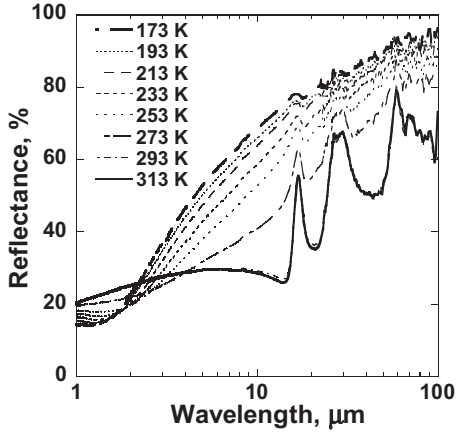

Fig. 4. Temperature dependence of spectral reflectance of SRD between 173 and 313 K.

because the temperature dependence of the optical properties of the candidate materials for the multilayer films is negligible when compared to that of the SRD.

4. EXPERIMENTAL RESULTS AND DISCUSSION

Two main features are required for the multilayer films of the SRD. First, the reflectance for the solar radiation is large, i.e., the α_S is small. Second, the transmittance of the infrared radiation from the SRD has to be sufficiently large in order to maintain the large variation in ε_H of the SRD, that is, it is necessary for $\Delta\varepsilon_H$ to be 0.40. The α_S of the SRD was found to be too large in the present study; its value was 0.81. Therefore, the α_S was set to be 0.20 and the $\Delta\varepsilon_H$ was set at 0.40 between 173 and 313 K. The sequence of the materials and the thickness of the multilayer films with the desired thermal radiative properties, $\alpha_S = 0.20$ and $\Delta\varepsilon_H = 0.40$, were searched for by changing the coded strings of the individual represented by Eq. (1) in the optimization process of the GA. In this present study, we defined that a good individual, who had properties close to the desired $\Delta\varepsilon_H$ and α_S, was assigned a high fitness value. The ε_H and α_S were calculated by using Eqs. (4) and (5).

As a result of the optimization, multilayer film with the desired thermal radiative properties was obtained. The structure of the multilayer film designed by this method was relatively simple. Only three materials were selected from the candidate materials. The multilayer film is nine

layers and consists of a-Si, Ge, and MgF_2. The optimum thickness of each layer was simultaneously determined. The calculated α_S and $\Delta\varepsilon_H$ of the SRD with the designed multilayer film were 0.24 and 0.40, respectively. In accordance with the result of the design based on the GA, the designed multilayer film was evaporated on the surface of the SRD by the electron beam evaporation method. In the following sections, calculated and measured results of the SRD with the designed multilayer film are presented.

4.1. Solar Absorptance α_S

The α_S was measured by using a spectroscope and an integrating sphere. A detailed explanation and description of the measurement system are presented in Ref. 18.

Figure 5 shows the measured spectral reflectance of the SRD with and without multilayer film from 0.25 to 2.5 μm, and calculated results are also shown. The spectral reflectance of the SRD with the multilayer film becomes much higher than that of the SRD without the multilayer film over this whole spectral region. Because of the multiple reflections in the multilayer film, the spectral reflectance from 0.6 to 2.0 μm becomes particularly high. The measured spectral reflectance shifts to the smaller spectral region compared to the calculated value. This difference is attributed to the accuracy of the optical constants of the materials for the multilayer

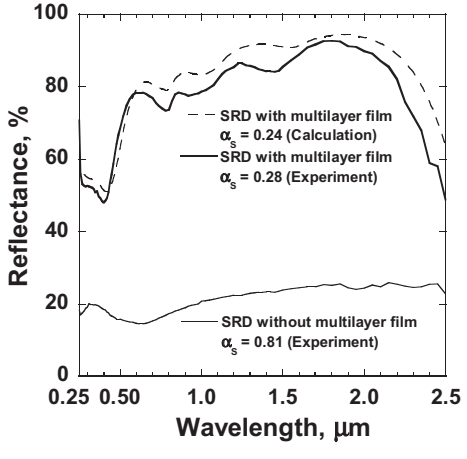

Fig. 5. Comparison of the spectral reflectance of the SRD with and without multilayer film in the spectral region of 0.25 to 2.5 μm.

films and the thickness of each layer. However, the calculated and measured α_S of the SRD with multilayer film are 0.24 and 0.28, respectively. Thus, the measured results for the SRD with the multilayer film shows good agreement with the calculated results. The multilayer film could sufficiently reduce α_S of the SRD from 0.81 to 0.28. Because of the restrictions of maintaining the value of $\Delta\varepsilon_H$ and using the evaporation technique, this value represented the best reduction of α_S in the present study.

4.2. Total Hemispherical Emittance ε_H

The temperature dependence of ε_H of the SRD was measured by the calorimetric method between 173 and 373 K. A detailed explanation of the calorimetric method and description of the measurement system are presented in Ref. 2.

Figure 6 shows the calculated and measured ε_H of the SRD with the multilayer film along with ε_H of the SRD without the multilayer film. Because of the slight absorption of the multilayer film, the ε_H of the SRD with the multilayer film was larger than that of the SRD without the multilayer film over the entire temperature range. The measured ε_H is 0.76 at 313 K and 0.36 at 173 K. The range of the variation in ε_H is 0.40 between 173 and 313 K. The maximum variation in ε_H is 0.42 between 173 and 373 K. The measured results agree well with the calculated results. The

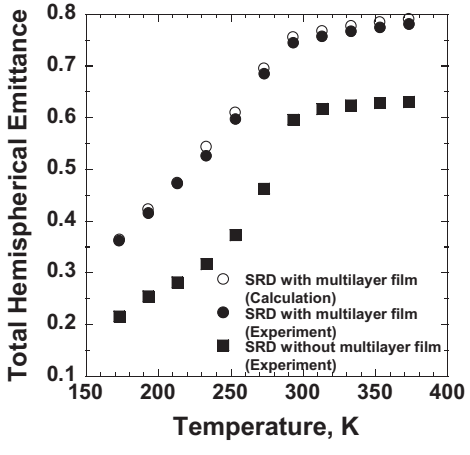

Fig. 6. Comparison of the temperature dependence of ε_H of the SRD with and without multilayer film.

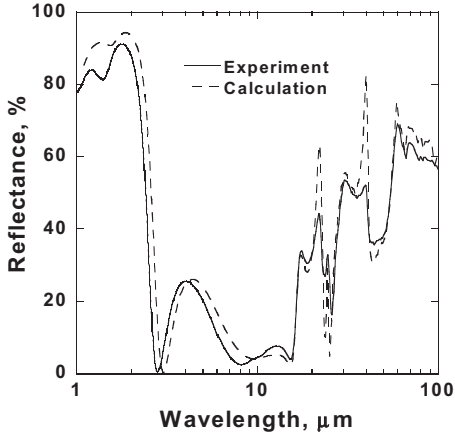

Fig. 7. Comparison of the calculated and measured spectral reflectance of the SRD with multilayer film in the spectral region of 1.0 to 100 μm at room temperature.

maximum deviation of the experimental results from the calculated results is approximately 0.02 at 233 K.

Figure 7 shows the calculated and measured spectral reflectances of the SRD with the multilayer film at room temperature in the spectral region of 1.0 to 100 μm. The spectral reflectance of near-normal incidence was measured by use of a Fourier transform spectroscope (Bio-Rad: FTS-60A/896). The measured spectral reflectance shifts to a smaller spectral region compared to the calculated value below 10 μm. The strong absorptions at 25 and 45 μm are attributed to the influences of the optical phonons of MgF_2 in the multilayer film, but the magnitudes of the peak and valley of the measured spectral reflectance at 25 and 45 μm are different from the calculated values. It is considered that the optical constants and homogeneity of MgF_2 are affected and changed in the evaporation

Table I. Comparison of α_S and $\Delta\varepsilon_H$ (173 to 313 K) of the SRD With and Without Multilayer Film

	α_S	$\Delta\varepsilon_H$
SRD without designed multilayer film (Experiment)	0.81	0.40
SRD with designed multilayer film (Calculation)	0.24	0.40
SRD with designed multilayer film (Experiment)	0.28	0.40

process. The influence of the thickness of each layer on ε_H is smaller than that on α_S since the thickness of each layer is sufficiently small compared to the wavelength of infrared radiation. From these results, it was recognized that the designed multilayer film maintained the large variation in ε_H of the SRD. The results are summarized in Table I.

5. CONCLUSIONS

The thermal radiative properties of the SRD and design method of the multilayer films for the SRD were presented in this paper. Calculations of the thermal radiative properties of multilayer films were carried out by use of the optical constants of the materials. In order to reduce the high solar absorptance of the SRD, multilayer films were designed by using a genetic algorithm (GA). A GA simultaneously determined the optimum thickness and sequence of the materials of multilayer film with desired thermal radiative properties. The designed multilayer film was nine layers and consisted of only three materials, i.e., a-Si, Ge, and MgF_2. The multilayer film was evaporated on the surface of the SRD by the electron beam evaporation method. The experimental results of α_S and ε_H of the SRD with the multilayer film showed good agreement with the calculated results. Reduction of the α_S of the SRD became possible with the multilayer films. Moreover, the ε_H maintained the range of the variation of ε_H of the SRD.

ACKNOWLEDGMENTS

We would like to thank A. Okamoto, Y. Nakamura, Dr. Y. Shimakawa, T. Mori, and A. Ochi of NEC Corporation for sample preparation.

REFERENCES

1. S. Tachikawa, A. Ohnishi, K. Shimazaki, A. Okamoto, Y. Nakamura, Y. Shimakawa, M. Kosaka, T. Mori, and A. Ochi, *SAE Technical Paper No. 00ICES-314* (2000).
2. K. Shimazaki, S. Tachikawa, A. Ohnishi, and Y. Nagasaka, *High Temp.-High Press.* **33**:525 (2001).
3. L. Li and J. A. Dobrowolski, *Appl. Opt.* **31**:3790 (1992).
4. J. A. Dobrowolski and R. A. Kemp, *Appl. Opt.* **29**:2876 (1990).
5. D. E. Goldberg, *Genetic Algorithms in Search, Optimization, And Machine Learning* (Addison–Wesley, Reading, Massachusetts, 1989).
6. Y. Tokura, A. Urushibara, Y. Moritomo, T. Arima, A. Asamitsu, G. Kido, and N. Furukawa, *J. Phys. Soc. Japan* **63**:3931 (1994).
7. A. P. Ramirez, S.-W. Cheong, and P. Schiffer, *J. Appl. Phys.* **81**:5337 (1997).
8. A. Urushibara, Y. Moritomo, T. Arima, A. Asamitsu, G. Kido, and Y. Tokura, *Phys. Rev.* **51**:14103 (1995).
9. G. H. Jonker and J. H. van Santen, *Phys.* **16**:337 (1950).

10. D. G. Li and A. C. Watson, *Proc. 1997 IEEE Int. Conf. Intelligent Processing Systems* (1997), pp. 132–136.
11. R. Horikoshi, Y. Nagasaka, and A. Ohnishi, *Int. J. Thermophys.* **19**:547 (1998).
12. O. S. Heavens, *Optical Properties of Thin Solid Films* (Dover Pubs., New York, 1991), pp. 46–95.
13. M. P. Thekaekara, *The Solar Constant and the Solar Spectrum Measured from A Research Aircraft*, NASA TR R-351 (1970), pp. 71–80.
14. D. M. Roessler, *Brit. J. Appl. Phys.* **16**:1119 (1965).
15. K. Shimazaki, S. Tachikawa, A. Ohnishi, and Y. Nagasaka, *Int. J. Thermophys.* **22**:1549 (2001).
16. K. Shimazaki, S. Tachikawa, A. Ohnishi, and Y. Nagasaka, *Proc. 6th Asian Thermophys. Prop. Conf.* (Guwahati, India, 2001), pp. 182–187.
17. E. D. Palik, *Handbook of Optical Constants of Solids I-III* (Academic, New York, 1998).
18. A. Ohnishi and T. Hayashi, *Proc. Int. Symp. Environmental and Thermal Systems for Space Vehicles*, Toulouse, France (1983), pp. 467–470.